

NOISE PERFORMANCE OF THE GANYMEDE LASER ALTIMETER RECEIVER

T. Behnke¹, R. Kallenbach¹, M. Fuji², M. Kobayashi³, Y. Sato², K. Enya⁴, C. Hüttig¹, A. Stark¹, S. DelTogno¹, C. Althaus¹

¹DLR Institute for Planetary Research, Berlin, Germany, ²Meisei Electric Co. Ltd, Isesaki, Japan, ³Chiba Institute of Technology, Tokyo, Japan, ⁴Institute of Space and Astronautical Science, Japan Aerospace Exploration Agency, Yoshinodai 3-1-1, Sagami-hara, Kanagawa 229-8510

ABSTRACT

We report here on qualification and calibration test results demonstrating the science performance of the Avalanche Photodiode (APD) detector of the Ganymede Laser Altimeter (GALA, Fig. 1). Most importantly, the measures for noise reduction of the analogue receiver electronics are described. This includes proper grounding of the APD module (EXCELITAS C30654) and filtering in its vicinity and the additional measures to isolate switching noise of the analogue-to-digital converters (ADCs) from the sensitive single-ended analogue sensor pre-amplifier electronics of the APD. Tests with realistic electron irradiation doses being representative for the environment of the Jovian magnetosphere and additional shielding measures have been performed in order to ensure that the dark-current noise level of the receiver does not increase significantly over the mission time.

1. THE GANYMEDE LASER ALTIMETER

The GALA instrument is intended to be launched in 2023 onboard ESA's JUICE spacecraft. It shall map, after a six-year space cruise, Ganymede's topography from spacecraft altitudes of nominally 500 km. Fig. 1 gives a schematic overview of the GALA TRU. A diode-laser pumped Nd:YAG laser emits pulses at 1064 nm wavelength with nominally 17 mJ energy (9×10^{16} photons) and 5 ns duration at repetition rates of 10 to 30 Hz, and during fly-bys, at reduced pulse energy, up to 50 Hz. The receiver (RX) telescope has an area of 0.03 m² and collects a small fraction of these photons scattered off Ganymede's surface, which has a diffuse reflectivity in the range of 0.3 to 0.7. Assuming a spacecraft altitude of 500 km, and an overall RX transmission of 0.77, at least 760 photons are transmitted onto the Si APD. Its quantum efficiency for photons at 1064 nm is 0.35, therefore, about 270 electron-hole pairs are generated within 5 ns corresponding to a return pulse of 10nA signal current. This is signal-to-noise ratio of 2 to 5 above the noise-equivalent power (NEP) specified by EXCELITAS for the C30659H APD, typical values are 0.2 pA/ $\sqrt{\text{Hz}}$ up to at most 0.6 pA/ $\sqrt{\text{Hz}}$ in a bandwidth of 100 MHz [1].

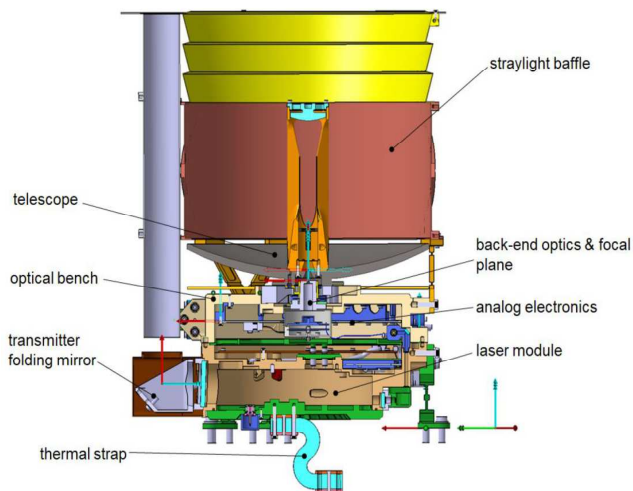


Figure 1. Top: The compact design of the GALA Transceiver Unit (TRU) [1] has been optimized for energetic-particle shielding of radiation-sensitive components such as the APD placed onto the focal plane in the centre of the instrument. The analogue active Q-switch electronics are located very close to the APD although their 10 ns switching spikes with amplitude 3 kV are electrically well shielded. The pump diode lasers are driven by current pulses with amplitude of 200 A that last about 70 μs . Bottom: Flight model of the GALA TRU on the test bench at Hensoldt Optronics in Oberkochen, Germany. Credit: DLR / Hensoldt Optronics / JAXA

2. RECEIVER NOISE CONSIDERATION

2.1 APD noise sources

The output signal current i_s from an APD equals

$$i_s = M * R_o(\lambda) * P_s \tag{1}$$

- M = gain (typ. 150)
- $R_o(\lambda)$ = responsivity (typ. 0.3 A/W, $M=1$)
- P_s = incident optical power

The detection is limited by the noise sources of the APD itself. NEP power (calculated in i_n) of the GALA detector according Eqs. 2 is in the range of 0.2 pA/ $\sqrt{\text{Hz}}$ up to at most 0.6 pA/ $\sqrt{\text{Hz}}$ in a bandwidth of 100 MHz.

$$i_n = \sqrt{2 * q * (i_{DS} + i_{DB} * M^2 * F) * B} \tag{2}$$

- i_{DS} = surface dark signal
- i_{DB} = bulk dark signal
- F = APD noise factor
- B = Bandwidth

2.2 TIA transfer function

A transimpedance (TIA) amplifier converts the signal current into a voltage. On a high impedance node to total current circulates through R_f .

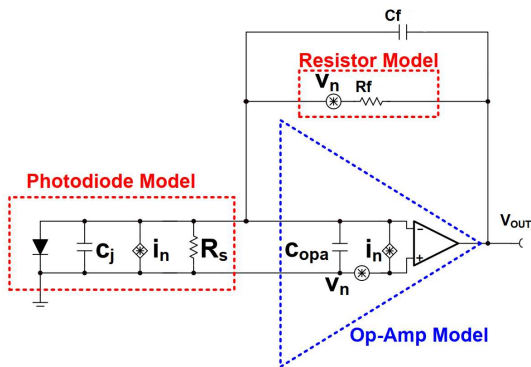


Figure 2. APD and TIA reduced model

Fig. 2 shows a transimpedance amplifier to convert the APD overall current into a voltage:

$$v_{out} = (i_s + i_n) * R_f \tag{3}$$

The total noise output voltage is calculated as quadratic sum of all noise components (APD and TIA). The noise transfer function of the TIA is given in Eqs. 4.

$$v_{out} = \frac{v_n + (i_n * R_f) + v_r + \frac{\omega^2}{\omega_0^2} v_n \left(\frac{C_f + C_{IN}}{C_f} \right)}{1 + \frac{\omega^2}{\omega_0^2}} \tag{4}$$

$$\omega_0^2 = \frac{1}{C_f^2 * R_f^2}$$

with $C_{IN} = C_j || C_{opa}$

The APD and TIA parasitic capacitors composes a pole. At low frequency $\omega < \omega_0$ the total output noise is dominated by the APD noise and thermal resistor noise of the feedback resistor R_f . If $\omega = \omega_0$ we see a peaking of the noise voltage. At higher frequency $\omega \gg \omega_0$ the process decay with -20 dB/decade. Simulation results with realistic capacitor parameters is given in Fig. 3.

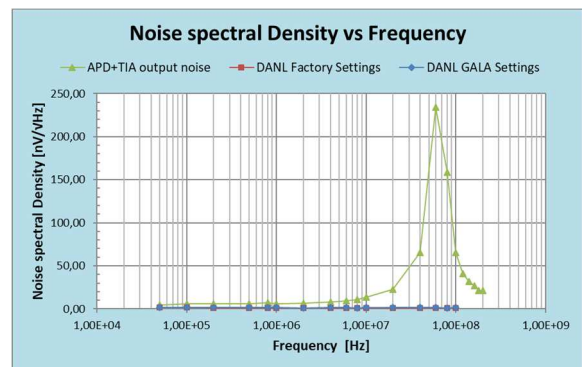
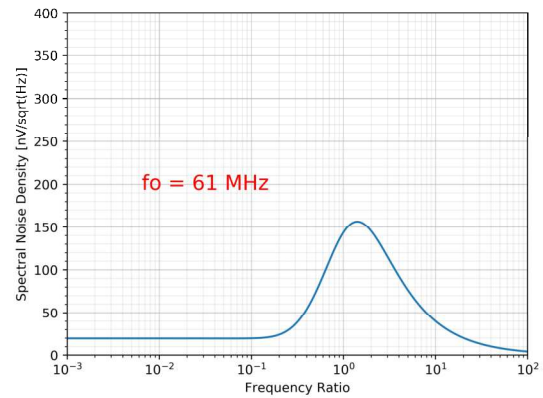


Figure 3. Modelling and test results of APD output noise

The noise peaking is strong coupled with the manufacture process of the APD and TIA and differs between a hybrid chip on board technology (i.e. Si dies mounted and bonded on a ceramic) or a monolithic architecture based on separate components mounted on a FR4 PCB. Furthermore the peaking is dominated by the parasitic capacitors C_{IN} and C_f . The low frequency spectral noise density is 12 nV/ $\sqrt{\text{Hz}}$ referred to the output port of the transimpedance amplifier (TIA) of the APD module (Fig. 4). For testing and data evaluation we use the low noise TEKTRONIX RSA5103B Real Time Signal Analyzer.

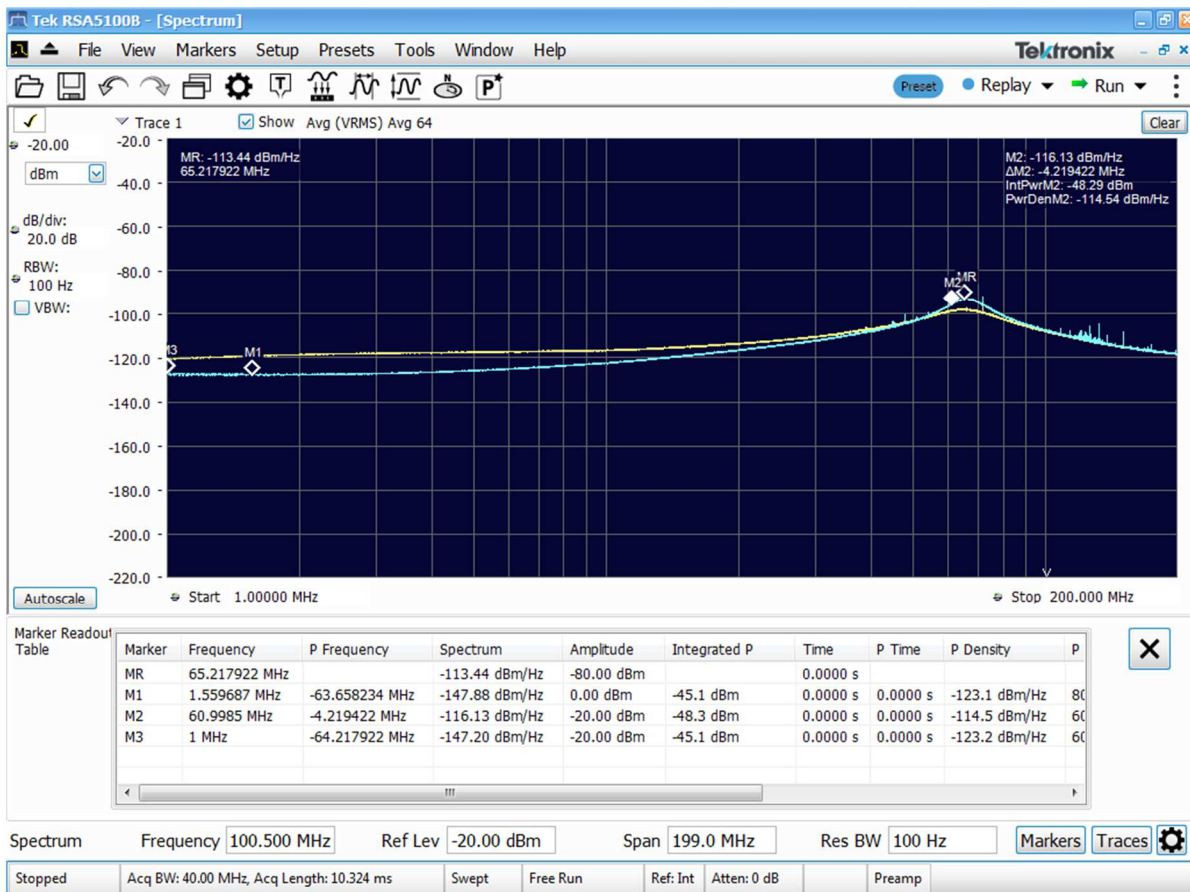


Figure 4. Reference measurement with single APD, yellow: low HV bias (10 V), turquoise: APD with high voltage = 351 V

Aground the division of work with our Japanese team a complete hybrid APD/TIA focal plate module and the front-end Analogue Electronics Module (AEM) was available during GALA EM/EQM integration phase. Now, first results must be double-checked and additional noise sources considered (Fig. 6).

2.3 EMI induced noise by front end signal processing

In the GALA instrument the APD is aligned inside the Transceiver Unit behind the telescope close to the high power switched diode laser. The front end electronic AEM consists of two operational amplifiers with a fixed gain. Gain switching between high and low gain is realized by an attenuator in front of the amplifier stage. The transformation to a full differential balanced signal

ensures high common mode noise immunity and best signal integrity in case of ground bounce.

Two 100 MHz 180° phase shifted 12 bit ADCs digitizes the analogue APD signal. The conversion factor amounts to 1V/2048 DN. Three clock domains, 40 MHz for FPGA clock domain, 2 MHz high voltage APD power supply and an extern 100 MHz ADC sampling clock, are active during APD operation. Tests in the closed AEM compartment show a strong coupling of spurious spectral errors into the APD signal. The interference injection was strong coupled with the operation of the ADCs. The AEM layout was designed according HF guidelines with a low impedance common ground plane and a multiple point grounding along the PCB border to the AEM housing.

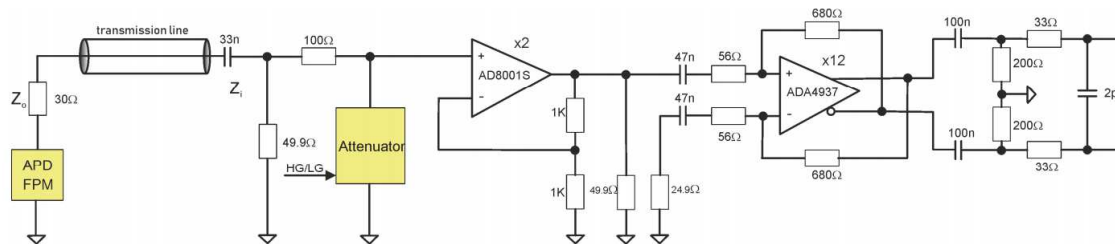


Figure 5. GALA APD Signal Chain Architecture

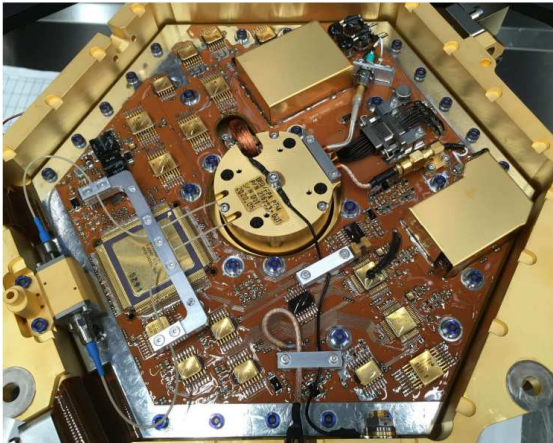


Figure 6. Analogue Electronics Module in flight configuration before rework

Further investigation shows that radiated emission of the 100 MHz clock from active ADCs into the shielded analogue signal section could be identified as root cause. The ADC (aggressor) injects over the metallic surface in the closed compartment electro-magnetic radiation into AEM metallic shielded analogue signal chain. Additional tests show also a strong interaction between the ground reference of the single ended APD signal and the ground plain of the signal chain. Root cause is the inductive portion of the ground interconnection between TIA ground and AEM ground.

The result is shown in Fig. 7. The closed housing acts as resonating cavity. The effect is only visible, if the two ADCs in operation mode. The presence of the clock alone shows no extensive signal distortion (Fig. 8)

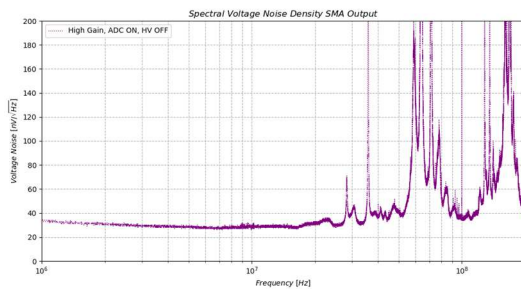


Figure 7. Effect of radiated emission into APD signal during ADCs ON

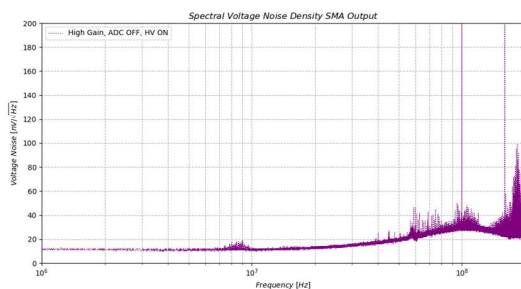


Figure 8. Effect of radiated emission into APD signal during ADCs OFF

Workaround was an additional extensive metallic foil over the sensitive area to provide additional high frequency low impedance grounding. The sensitive area is protected against radiated emission and the distortions disappears. Due to the conformal coating of the ADCs a direct shielding of the converter was unfeasible.

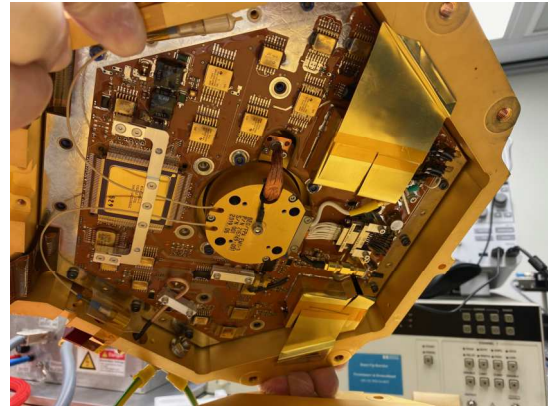


Figure 9. Analogue Electronics Module with APD housing in centre and extra shielding (Kapton taped). The picture shows the practical implementation on AEMI-3 model.

The overall noise performance after final flight-like implementation is shown in Fig. 10. The plot shows the spectrum at the technological output port of the APD signal. This port is accessible during the entire AIV flow.

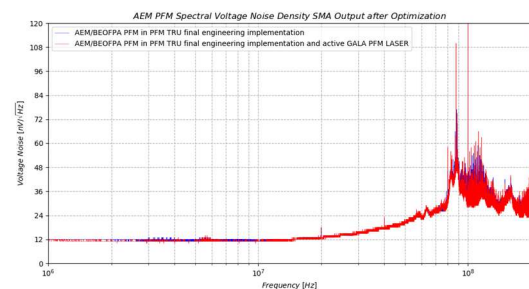


Figure 10. Final Noise Spectral Density of GALA Detector (APD)

Strong peak at 100 MHz is impact of the fundamental ADC sampling frequency into the input signal. During operation the input impedance of the ADC is changing between sample and hold stage.

The two channels 12 bit parallel data bus is connected to the Rangefinder Module (RFM). For synchronisation reasons the 100 MHz sampling clock is output of the RFM and driven over a 2m twisted shield differential signal cable bundle (LVDS). The reduced spectral cleanliness of the sampling clock, jitter and aberration from ideal 50% duty cycle shows few prominent frequencies in the spectral range up to 200 MHz. The assumption is a direct coupling of clock portion into the analogue signal if the clock amplitude of the ADC is in the critical voltage threshold between sample and hold. The peaking as discussed before is visible as intrinsic

curve. The overall performance is close to the theoretical limits.

Fig. 10 shows the noise floor at the TIA output just before the analogue signal chain. Further investigation was done in the digital domain after digitalization of the analogue APD signal. Fig. 11 shows noise spectral density of the GALA APD sensor (EXCELITAS C30654) within an FFT bandwidth of 100 MHz after analogue amplification and digitization by two ADCs 9254S. The noise peaks at 48 MHz and 58 MHz are due to switching noise of the ADCs. This noise has been reduced by about a factor 5 by low-inductive additional grounding of the analogue pre-amplifiers in the Analog Electronics Module (AEM).

The peaking in the higher frequency range as shown in Fig. 10 is compensated by the frequency response of the amplifier stage and the input filter of the ADC converter at higher frequency.

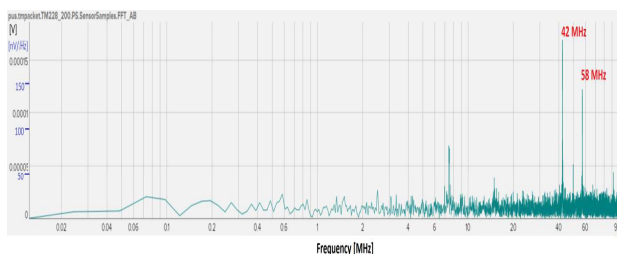


Figure 11. FFT plot of digitized APD signal

The noise compensation in the peaking region as seen in Fig. 11 is chosen to optimize the signal detection and is a compromise between reduced gain bandwidth and increased noise.

2.4 EMI induced noise by high power laser operation

During laser operation GALA detects no crosstalk of any 200 A pumping pulse, duration 50 μ s neither the 3 kV 10 ns active Q-switch pulse with repetition rate of up to 30 Hz within the analogue APD signal. For details refer to Fig. 10 and Fig. 11. The GALA grounding concept is strong split between receiver ground and transmitter ground. In combination with the secondary multipoint grounding concept HF currents find the lowest impedance return path over the chassis to S/C ground. The blue trace shows the spectral noise density without laser operation, whereas the red trace shows noise spectral density during emitting laser pulses. The implementation of isolated ground planes, the concept of multipoint grounding and the differential signal concept as well for the laser return signal as the differential gate driver for the active Q-switch provides high signal integrity and low signal distortion.

It could be verified by test that the laser operation contributes no noticeable portion to the overall noise budget.

As example Fig. 12 shows the GALA SpW communication signals during laser firing (top) and the corrupted signal integrity on a common ground referenced laser system (BELA) on the bottom [2], [3].

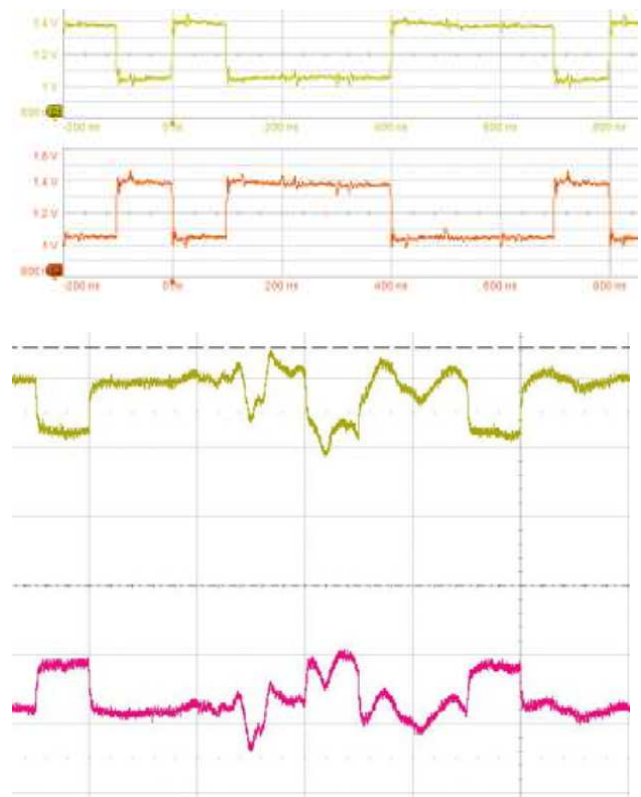


Figure 12. SpW signal integrity (LVDS) on different ground architecture. Top: receiver and transmitter separation (GALA) Bottom: common ground referenced laser system (BELA)

Note, the ratio between signal current of 10 nA and 200 A amounts to 10 decades. Both compartments are close together as part of the TRU unit.

3. PERFORMANCE AFTER RADIATION

Tab. 1 shows noise spectral density of the GALA APD sensor (EXCELITAS C30654) at several frequencies after irradiation. Total non-ionizing dose (TNID) causes displacement damage and consequently increase of bulk dark current, which is more important than surface dark current in the detection bandwidth of GALA from 100 kHz to 100 MHz. After additional shielding the TNID level at the location of the APD sensor is expected to 1.3×10^7 MeV/g only.

Table 1. Noise spectral density after radiation

APD#	TID	TNID	Noise spectral density [nV / $\sqrt{\text{Hz}}$] at frequency [MHz]				
			0.1	1	10	50	100
C4864	None	None	9	12	33	84	65
C4930	3.6 kRad Protons	10^8 MeV/g	24	24	52	147	75
C4943	30 kRad Electrons	8.8×10^8 MeV/g	39	35	74	162	66

4. SUMMARY

Three major goals have been achieved during the development of the GALA Receiver electronics:

The laser transmitter electronics noise contributes less than $10 \text{ nV}/\sqrt{\text{Hz}}$ up to a bandwidth of 88 MHz to the APD sensor noise. This bandwidth corresponds to rise times of 4 ns which is approximately the pulse width of the laser transmitter. Typical return pulses from Ganymede's surface range between 15 ns to 35 ns width depending on the surface slope and roughness.

The typical noise equivalent power of the digitized sensor data is $12 \text{ nV}/\sqrt{\text{Hz}}$ up to a bandwidth of 100 MHz referred to the output port of the transimpedance amplifier (TIA) of the APD module (Fig. 10). This corresponds to the theoretical noise limit of $23 \text{ nV}/\sqrt{\text{Hz}}$ of the $33 \text{ k}\Omega$ feedback resistor of the TIA multiplied by the voltage division ratio of 50/87 of the output stage. The so-called "peaking" in the sensor's transimpedance amplifier is compensated by the frequency response of the analogue pre-amplifiers before digitization. This leads to a rather flat responsivity curve in a bandwidth of 100 MHz with the specified responsivity value of 750 kV/W .

The noise of the receiver will not increase significantly during the mission time (Tab. 1) after additional shielding of the APD sensor had been implemented.

The ADC clock distribution over a long distance is crucial. For further improvement the application of a sine clock, a compact data interface (C-Link), or an additional synchronisation between source (AEM) and receiver (RFM) is recommended.

5. REFERENCES

- [1] H. Hussmann, K. Lingenauber, R. Kallenbach, J. Oberst, K. Enya, M. Kobayashi, N. Namiki, J. Kimura, N. Thomas, L. Lara, G. Steinbrügge, A. Stark, F. Luedicke, Kai Wickhusen, T. Behnke, C. Althaus, S. DelTogno, B. Borgs, H. Michaelis, J. Jänchen, and the GALA Team, "The Ganymede Laser Altimeter (GALA)," in *EPSC Abstracts*, Vol. 11, EPSC2017-567-4, 2017, European Planetary Science Congress, Riga, Latvia, 2017.
- [2] Kallenbach, R., Behnke, T., Perplies, H., Henkelmann, R., Rech, M., Geissbühler, U., Péteut, A., Lichopoj, A., Schroedter, R., Michaelis, H., Seiferlin, K., Thomas, N., Castro, J.M., Herranz, M., Lara, L., "Electromagnetic Compatibility of Transmitter, Receiver, and Communication Port of a Space-Qualified Laser Altimeter," 2016 ESA Workshop on Aerospace EMC, *IEEE Xplore*, DOI: 10.1109/AeroEMC.2016.7504591
- [3] Thomas, N., Spohn, T., Barriot, J.-P., Benz, W., Beutler, G., Christensen, U., Dehant, V., Fallnich, C., Giardini, D., Groussin, O., Gunderson, K., Hauber, E., Hilchenbach, M., Iess, L., Lamy, P., Loral, L.-M., Lognonné, P., Lopez-Moreno, J.J., Michaelis, H., Oberst, J., Resendes, D., Reynaud, J.-L., Rodrigo, R., Sasakio, S., Seiferlin, K., Wiczorek, M. and Whitby, J. (2007). The BepiColombo Laser Altimeter (BELA): Concept and Baseline Design. *Planet. Space Sci.* **55**, 1398-1413.